Available online at www.sciencedirect.com
ScienceDirect
International Journal of Mass Spectrometry 266 (2007) 62–75
International Journal of Mass Spectrometry
www.elsevier.com/locate/ijms

Propagation of structural deviations of poly(amidoamine) fan-shape dendrimers (generations 0–3) characterized by MALDI and electrospray mass spectrometry

Rémi Giordanengo [a], Michaël Mazarin [a], Jiangyu Wu [b], Ling Peng [b], Laurence Charles [a,*]

[a] *Aix-Marseille Université, JE 2421, Marseille F-13397, France*
[b] *Département de Chimie, CNRS UMR6114, Marseille F-13288, France*

Received 6 March 2007; received in revised form 6 July 2007; accepted 6 July 2007
Available online 12 July 2007

Abstract

Fan-shape PAMAM dendrimers, from generations 0 to 3, were analyzed by mass spectrometry, using both MALDI and electrospray ionization techniques, to identify any structural deviations present in each sample. First, it could be concluded that all detected molecules were present in the samples as they were detected in MALDI as well as in electrospray mass spectra. Apart from commonly reported dendrimer defects ("missing arm" and "molecular loop"), new impurities were found to arise from propagation of these defects during the synthesis of upper generations. These assignments were based on both compound molecular weight and, when ions were detected with sufficient abundance, deviations from perfect structure behaviour during MS/MS experiments. Since new impurities could be created, either from perfect or defective molecules, during each new generation dendrimer synthesis, models were built to predict the molecular weight of a compound as a function of its synthesis history and efficiently guide mass spectral interpretation.

Keywords: PAMAM dendrimer; Defect propagation; Electrospray; MALDI; Predictive model

1. Introduction

Dendrimers are perfectly structured molecules with large numbers of cascade-branched units emanating from a focal point, resulting in densely packed end groups at the molecular surface [1–5]. Two main strategies can be used to synthesize such macromolecular structures. In the convergent approach [6], dendritic wedges are first prepared separately and then connected to a central core. The large structural differences between the perfect structure and eventual by-products, in which one or more dendritic wedges are missing, make purification relatively facile [7]. However, convergent strategies are generally limited to the construction of lower generations due to nanoscale steric issues [8]. In contrast, the divergent approach [9] allows the synthesis of very high generation dendrimers but suffers from a number of statistical defects. The divergent method involves a two-step iterative reaction sequence that produces concentric shells of branches around a central initiator core. In PAMAM synthesis, a Michael addition of methyl acrylate to an amine-terminated core is followed by the amidation of the resulting methyl ester derivatives with diethylamine to regenerate the terminal amines. Each iteration of the reaction sequence leads to the formation of the next generation. Three main types of side reactions may occur during the synthesis and have been described to produce defective structures detected as impurities in all generations [10–14]. The "missing arm" defect results from subquantitative success of the Michael addition or from the retro-Michael reactions occurring in dendrimer solutions. "Molecular loop" is due to intramolecular cyclization and may occur during the amidation step as ethylene diamine is a bifunctional reactant. Dimers may also form during the amidation step. Isolation of defect-free molecules is tedious since the dendrimer sample contains compounds of very similar structure and molecular weight [8]. Alternatively to sample purification, synthetic strategies could be improved. For example, the equilibrium between the Michael reaction and its retro version was

* Corresponding author. Tel.: +33 4 91 28 86 78; fax: +33 4 91 28 28 97.
E-mail address: laurence.charles@up.univ-mrs.fr (L. Charles).

1387-3806/$ – see front matter © 2007 Elsevier B.V. All rights reserved.
doi:10.1016/j.ijms.2007.07.002

shown to depend on temperature [15] and might therefore be optimized. Identification of defect molecules in each dendrimer generation is thus very useful to tentatively improve synthetic strategies.

Different analytical techniques can be used to investigate structural imperfections in dendrimers [16]. Amongst them, mass spectrometry (MS) has been thoroughly used for the characterization of dendrimer samples. Soft ionization techniques such as electrospray (ESI) and matrix-assisted laser desorption/ionization (MALDI) were shown to efficiently promote ionization of molecules in dendrimer samples such as PAMAM [4,10,12,14,15,17–19], poly(propylene imine) [20,21], poly(propylene amine) [22,23], poly(aryl ester) [24,25], carbosiloxane [26] and carbosilane [27–29], allowing the determination of dendrimer molecular weight and polydispersity. Both techniques were also employed to characterize metal complexes of dendrimers [30,31]. A quantitative model could be proposed to describe and predict dendrimer MALDI mass spectra [29]. When studying an entire series of macromolecules (up to generation 10), the extent of gas phase charging observed in ESI-MS was shown to be consistent with theoretical models predicting globular shape of dendrimers [7,13,32]. Mass-related information obtained in ESI or MALDI experiments indicate specific structural defects since imperfect molecules differ from the ideal expected structures by a known amount of mass. Structural deviations can also further be confirmed by collision-induced dissociations (CID) [7,33–36], surface-induced dissociations [22] or post-source decay (PSD) [35,37] experiments. As dendrimer molecular weight rapidly increases with the generation number, MALDI produces less complicated mass spectra than ESI, due to multiple charging induced by the electrospray process. However, MALDI has sometimes been reported to induce reactions of dendrimers within the matrix, producing the same molecules as those which would arise from an incomplete synthesis [23,25,38].

In this study, MALDI was used in conjunction with ESI to identify impurities in four generations (G_0–G_3) of tri(ethylene glycol) derived PAMAM dendrimers. The tested molecules have a fan-shaped structure since dendrimer growth is promoted at only one end of tri(ethylene glycol) (Scheme 1). Such dendrimers were recently shown to form stable complexes with RNA molecules via electrostatic interactions and self-assembly

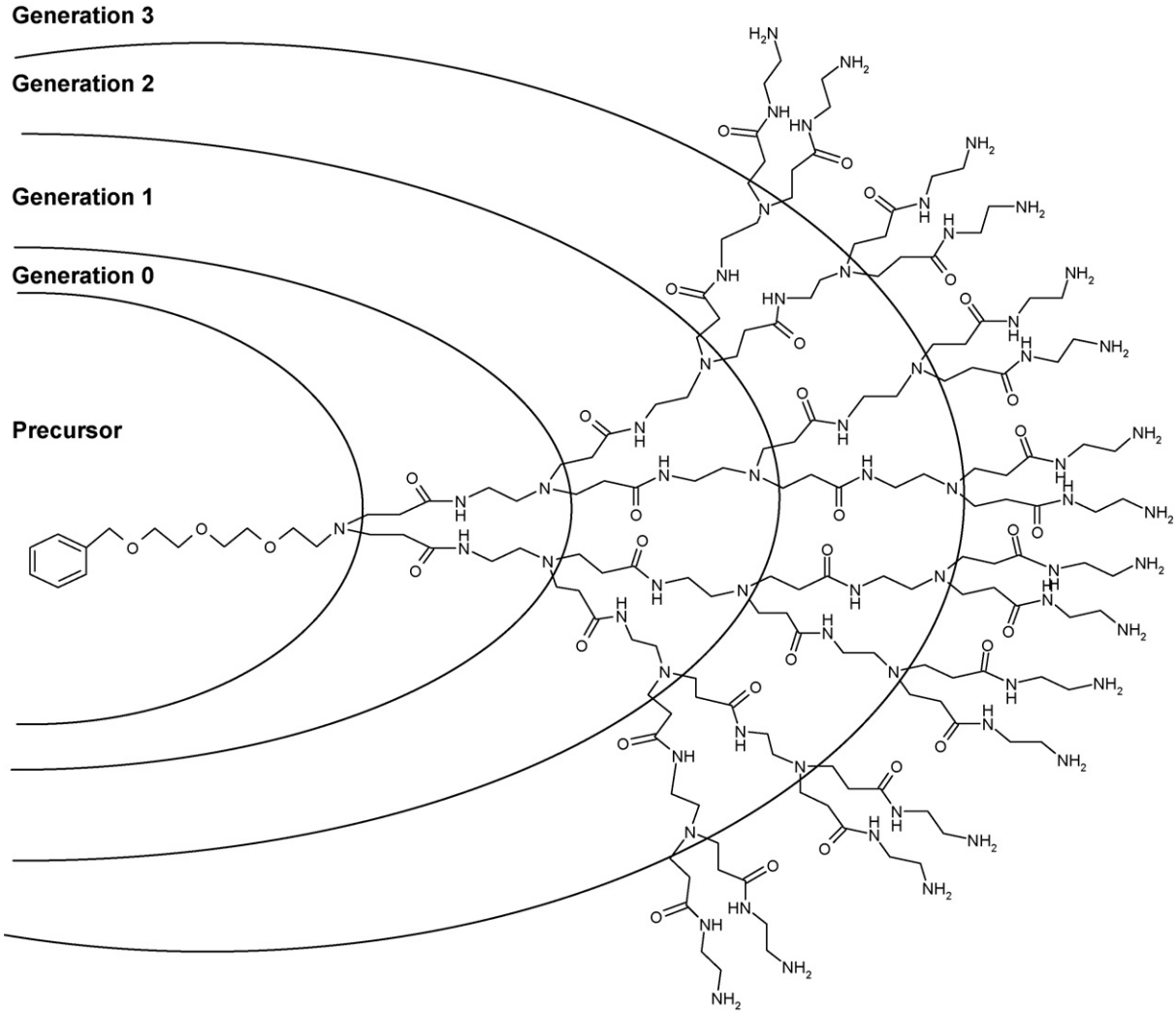

Scheme 1. Structure of PAMAM fan-shape dendrimer from generations 0 to 3.

process while leaving the other terminal of tri(ethylene glycol) chain accessible for targeting [19].

2. Experimental

2.1. Dendrimer synthesis

The synthesis of fan-shaped tri(ethylene glycol) derived PAMAM dendrimers has already been described elsewhere [19] and is briefly summarized hereafter. While one terminal hydroxyl group of tri(ethylene glycol) is selectively protected with a benzyl group, the other end is transformed to amine via successive tosylation, azidation and catalytic hydrogenation. The resulting compound (indicated as the dendrimer precursor in Scheme 1) is then submitted to a Michael addition with methyl acrylate to produce a diester molecule. Further treatment with ethylene diamine yields the generation 0 dendrimer, G_0NH_2. Further dendrimer generations are obtained using the conventional two-step iterative synthesis procedure: (a) branching double alkylation of terminal NH_2 groups with methyl acrylate followed by (b) amidation of the terminal ester with the corresponding diamine. No purification step was performed between each synthesis iteration. The crude product was dissolved in a small quantity of methanol and precipitated out by addition of ether. This final purification process was repeated three times and the resulting precipitate was dried under vacuum. Dendrimers are referred to as G_nNH_2, n indicating the generation number.

2.2. Chemicals

All chemicals were purchased from Sigma–Aldrich (St. Louis, MO). HPLC-grade solvents were from SDS (Peypin, France) and used as received. Deuterated methanol used in hydrogen/deuterium exchange experiments was from Eurisotop (Saint-Aubin, France).

2.3. Mass spectrometry

Electrospray experiments were performed using an API III Plus triple quadrupole mass spectrometer (Applied Biosystems SCIEX, Concord, Ont., Canada), equipped with an atmospheric pressure ionization (API) source. Ultra-high purity (UHP, 99.999%) nitrogen was used as the curtain gas in the API source (flow rate: 0.6 L min^{-1}) and zero-grade air as the nebulizing gas (flow rate: 0.8 L min^{-1}). The interface temperature was held at 54 °C. Positive mode ESI was performed at 5 kV and the orifice voltage was set at 35 V. The resolution for both quadrupoles was set at 0.7 u full width at half-height (FWHH). Tandem mass spectrometry (MS/MS) measurements were based on collision-induced dissociations (collision energies as indicated in the text), using UHP argon as the target gas, at a collision gas target of 75×10^{15} molecules/cm^2. The API III Hyperspec workstation and API software version 2.6 were used on a Power Macintosh 8100/80 for instrument control, data acquisition and data processing. Dendrimer solutions were prepared by dissolving 1–6 mg of dendrimer syrup in 200 μL of methanol and further diluted with a 3 mM ammonium acetate methanolic solution before electrospray ionization.

MALDI experiments were conducted with a Bruker autoflex reflectron TOF mass spectrometer equipped with a nitrogen laser emitting at 337 nm and with a 10 Hz frequency, a single-stage pulsed ion extraction source and dual microchannel plate detectors (Bruker Daltonics, Leipzig, Germany). The ion source and reflector potentials were set at 19.0 and 20.0 kV, respectively.

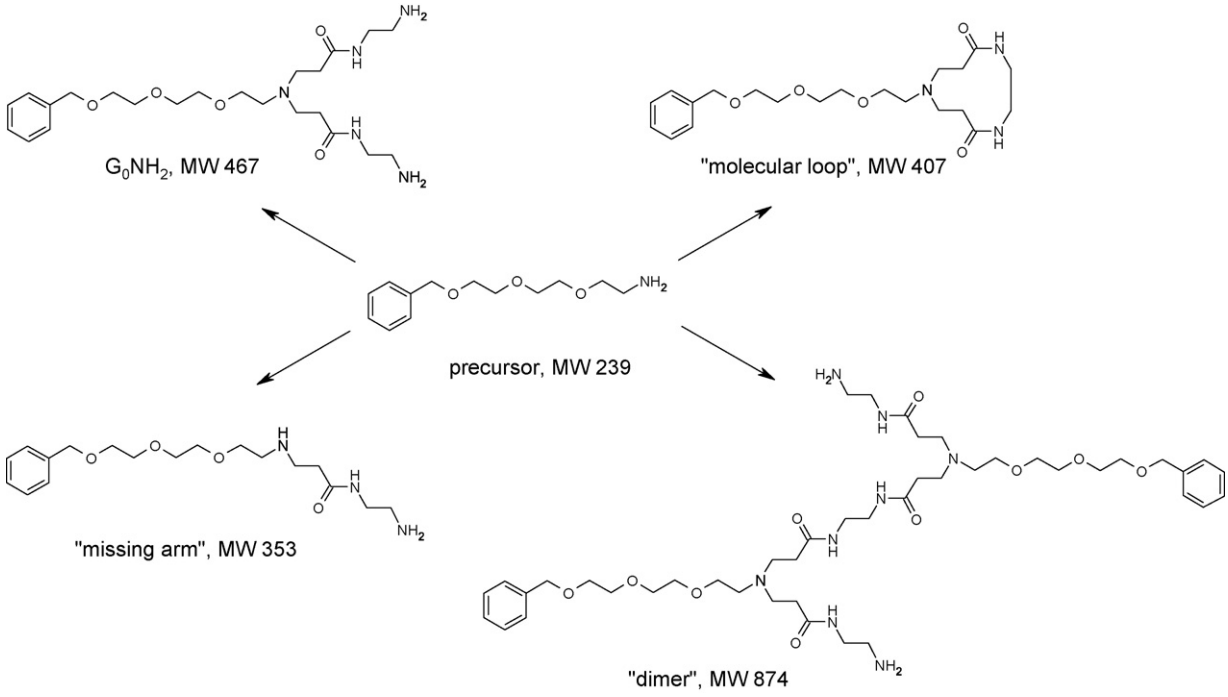

Scheme 2. Structure of the dendrimer molecule and the associated by-products expected in generation 0 sample.

Positive ion mode was used for all analyses. The delay time used in delayed extraction mode was optimized based on the polymer mass range and was generally 500 ns. MALDI samples were prepared by mixing 2,5-dihydroxybenzoic acid and the dendrimer sample, both dissolved in methanol, to reach a 1000:1 molar ratio for G_0–G_2. A higher matrix-to-analyte molar ratio (5000:1), together with the addition of a sodium salt, were required to promote molecule ionization in G_3. A 1 μL of the mixture solution was then deposited on the target and allowed to air dry at room temperature.

3. Results and discussion

3.1. Characterization of PAMAM generation 0

Generation 0 sample was obtained after the dendrimer precursor had been submitted to the first reaction sequence and could contain, apart from the expected G_0NH_2 perfect structure, three molecules arising from synthesis "failures" (Scheme 2). MALDI and ESI mass spectra of generation 0 sample are presented in Fig. 1. An abundant protonated G_0NH_2 molecule was observed as an intense peak at *m/z* 468 in MALDI, together with the sodium and potassium adducts detected at *m/z* 490 and *m/z* 506, respectively (Fig. 1a). Additional peaks with very low signal-to-noise ratio could be attributed to protonated molecules of "dimer" (*m/z* 875), "molecular loop" (*m/z* 408) and "missing arm" (*m/z* 354). Although the same molecules were detected after electrospray ionization (Fig. 1b), signals attributed to defects were of a much higher intensity, as compared to MALDI. Signal-to-noise ratios measured for ions at *m/z* 354, *m/z* 408 and *m/z* 438 (doubly protonated "dimer") suggest the defective molecules are more ESI responsive as compared to MALDI. As previously reported [23], if quantitative information were to be drawn from MS spectra, very different conclusions would be reached from these two experiments regarding sample composition. Nevertheless, since the same compounds were detected in both ionization methods, it could be concluded that ions observed in the MALDI mass spectrum actually arise from molecules initially present in the dendrimer sample.

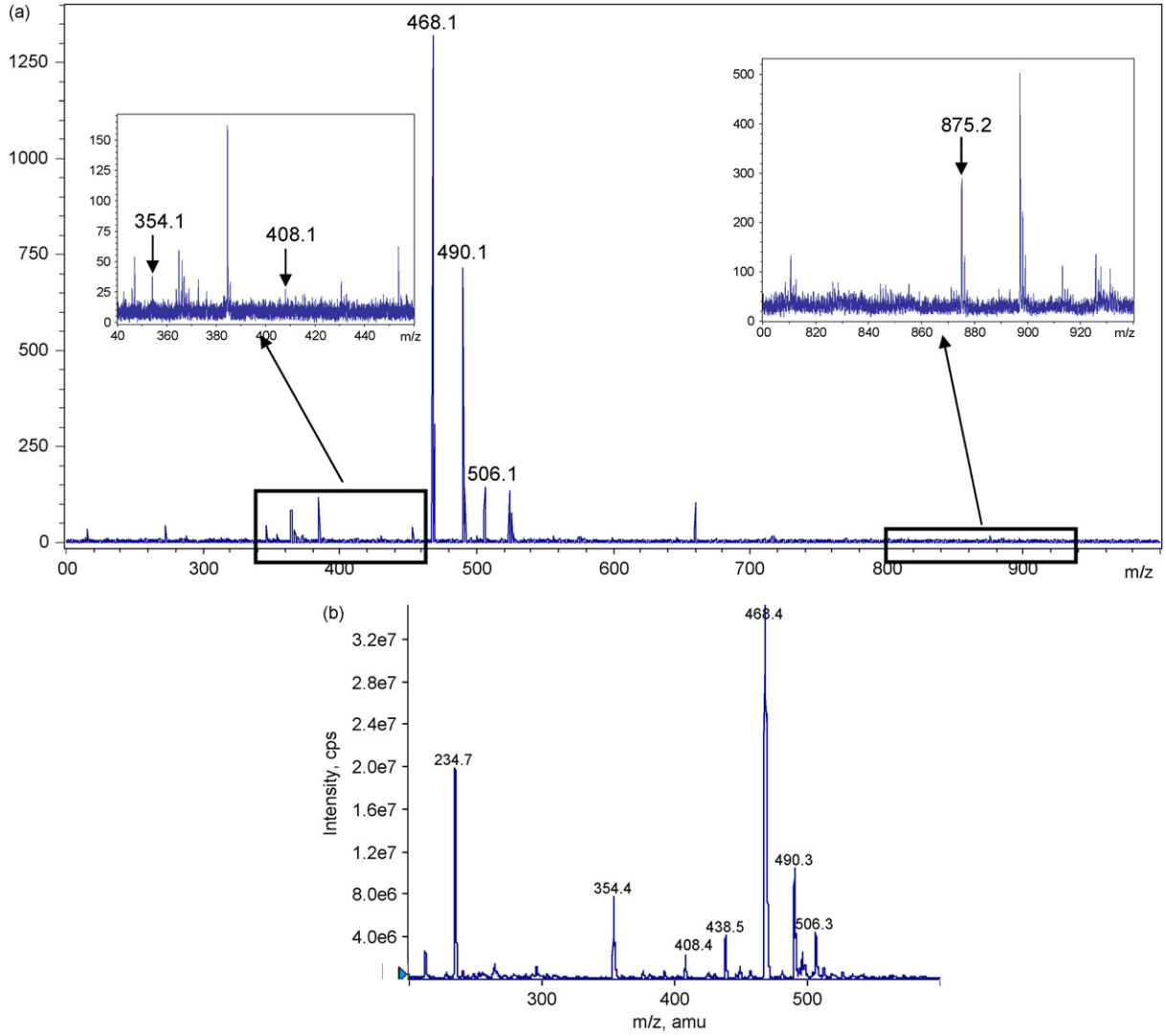

Fig. 1. Mass spectra obtained for generation 0 dendrimer sample (a) by MALDI (laser fluence: 35%; number of shots: 200) and (b) after electrospray ionization.

The behaviour of G_0NH_2 under collisional activation conditions was studied, to be further utilized as a reference to confirm the structure of defect ions. The MS/MS spectrum of *m/z* 468 is presented in Fig. 2. To account for the peaks observed at *m/z* 366 and *m/z* 252, a fragmentation route of protonated G_0NH_2 would consist of a two-step reaction in which consecutive neutral losses of, respectively 102 and 114 Da would occur (Scheme 3a). The elimination of an enol (namely, 1-(2-aminoethylamino)ethanol, 102 Da) from one arm of the dendrimer would be assisted by the presence of the second arm, leading to a six-membered cyclization to form *m/z* 366. A concerted mechanism would then allow this ring to be opened, resulting in the elimination of two neutral molecules, *N*-methylene-1,2-ethanediamine and ketene, that is a total mass of 114 Da. This particular mechanism was proposed amongst different possible others because it was supported by hydrogen/deuterium (H/D) exchange experiments where two peaks at *m/z* 369 and *m/z* 253 were observed in the MS/MS spectrum of fully deuterated precursor ion detected at *m/z* 475. An alternative route to produce *m/z* 252 would yield an intermediate at *m/z* 354 (Scheme 3b). In contrast to the mechanism

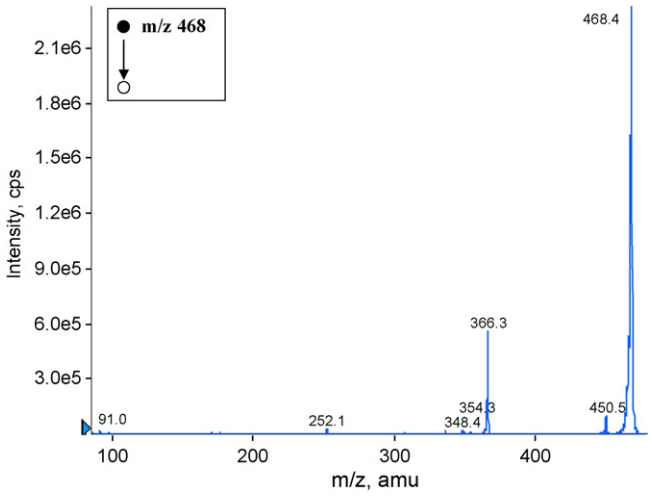

Fig. 2. ESI-MS/MS spectrum of the protonated G_0NH_2 (collision energy: 40 eV; laboratory frame).

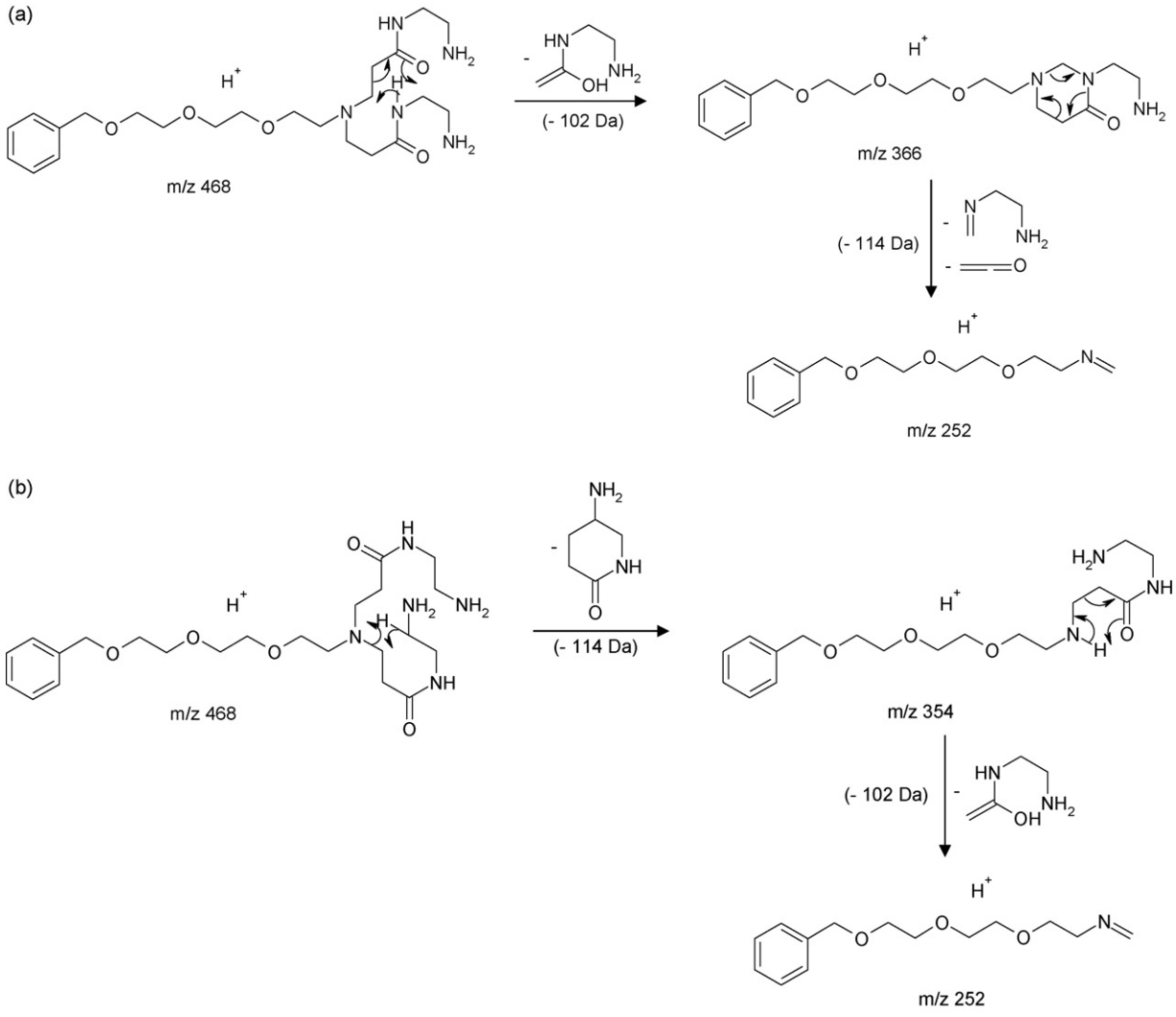

Scheme 3. (a) Proposed fragmentation reaction of $[G_0NH_2 + H]^+$ at *m/z* 468: the 102 Da neutral loss preceeds the 114 Da neutral loss. (b) Alternative fragmentation route of *m/z* 468: the 114 Da neutral loss occurs first and is followed by the 102 Da neutral loss.

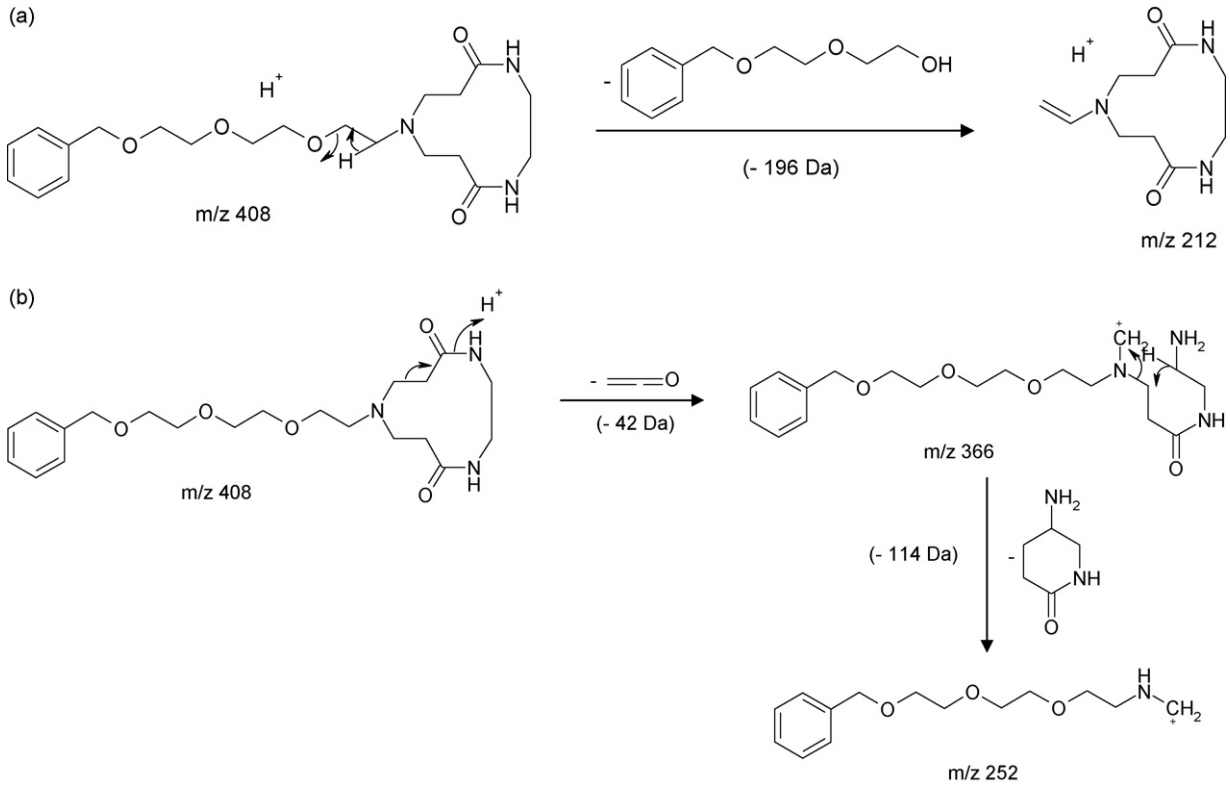

Scheme 4. Proposed fragmentation pathways of the protonated "molecular loop" to produce (a) *m/z* 212 daughter ion and (b) daughter ion detected at *m/z* 366 which would further dissociate to yield *m/z* 252.

in Scheme 3a, the 114 Da neutral would be a molecule of 5-aminopiperidin-2-one, obtained via a six-membered transition structure within one arm, and would occur prior to the 102 Da neutral loss. This consecutive enol elimination would no longer require the assistance of a second dendrimer arm in contrast to the mechanism depicted in Scheme 3a. The first reaction in Scheme 3b would occur at a slower rate than the dissociation described in Scheme 3a, as indicated by the much lower abundance of *m/z* 354 as compared to *m/z* 366. Proton bonding on the oxygen atom in the carbonyl group would induce the loss of a water molecule, as observed from *m/z* 468 and *m/z* 366 to yield *m/z* 450 and *m/z* 348, respectively. Finally, the peak detected at *m/z* 91 was attributed to a benzylium ion arising from a dissociation induced

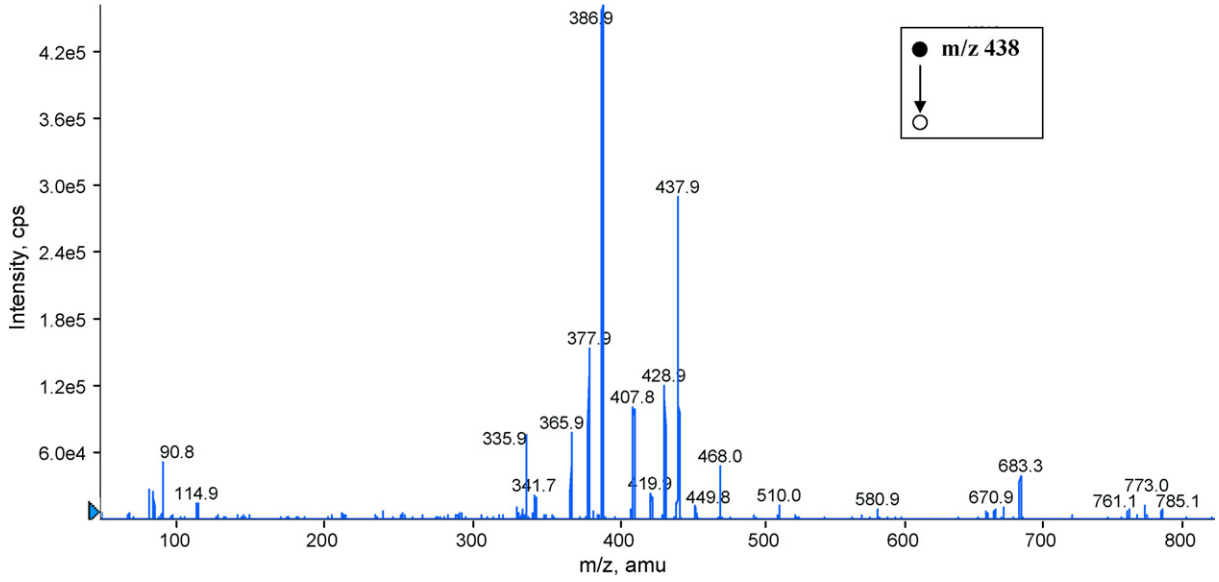

Fig. 3. ESI-MS/MS spectrum of the doubly protonated "dimer" in generation 0 sample (collision energy: 20 eV; laboratory frame).

by a proton binding on the first oxygen atom in the glycol chain.

Dissociation of defected molecules was then studied with regards to the fragmentation pattern of the perfect structure. The dissociation of the "missing arm" protonated molecule (*m*/*z* 354) lead to the formation of a daughter ion at *m*/*z* 252, according to the 102 Da neutral loss mechanism in Scheme 3b. The *m*/*z* 354 precursor ion was also observed to undergo water elimination as indicated by a low abundance daughter ion at *m*/*z* 336. Finally, a benzylium ion was detected at *m*/*z* 91.

Fragmentation mechanisms proposed to account for the ions resulting from the dissociation of the protonated "molecular loop" are described in Scheme 4. In contrast to the two previous molecules, the reaction yielding the most intense fragment detected at *m*/*z* 212 would result from a bond cleavage within the ethylene glycol moieties (Scheme 4a). Alternative dissociations of the precursor ion would occur upon ring opening. Binding of the proton on one of the secondary amino group in the "loop" would induce the loss of a ketene molecule to produce *m*/*z* 366 (Scheme 4b). According to mechanisms proposed in Scheme 3, no 102 Da neutral loss could be envisaged

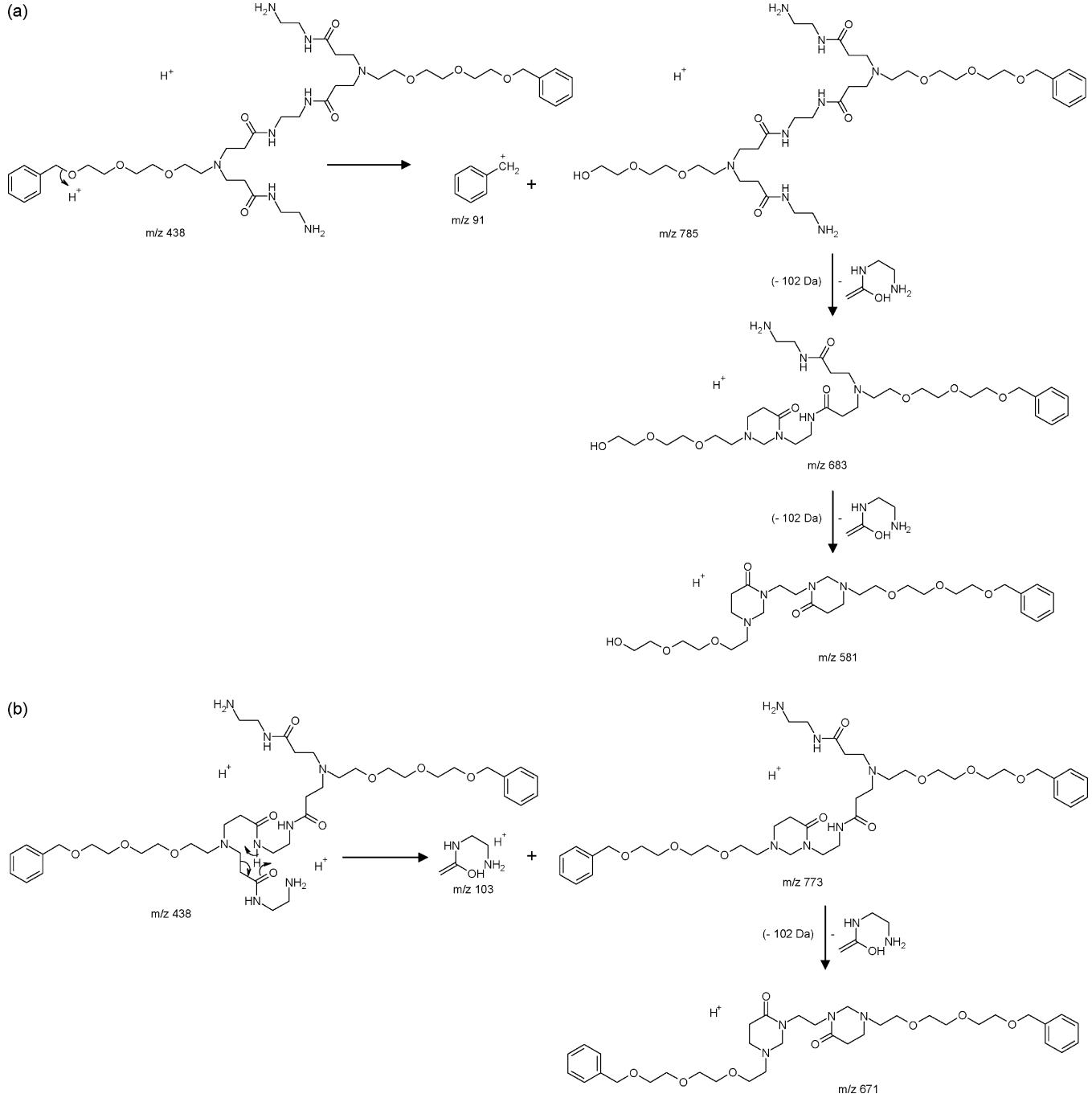

Scheme 5. (a)–(e) Proposed dissociation reactions yielding two singly charged products from the doubly protonated "dimer" at *m*/*z* 438.

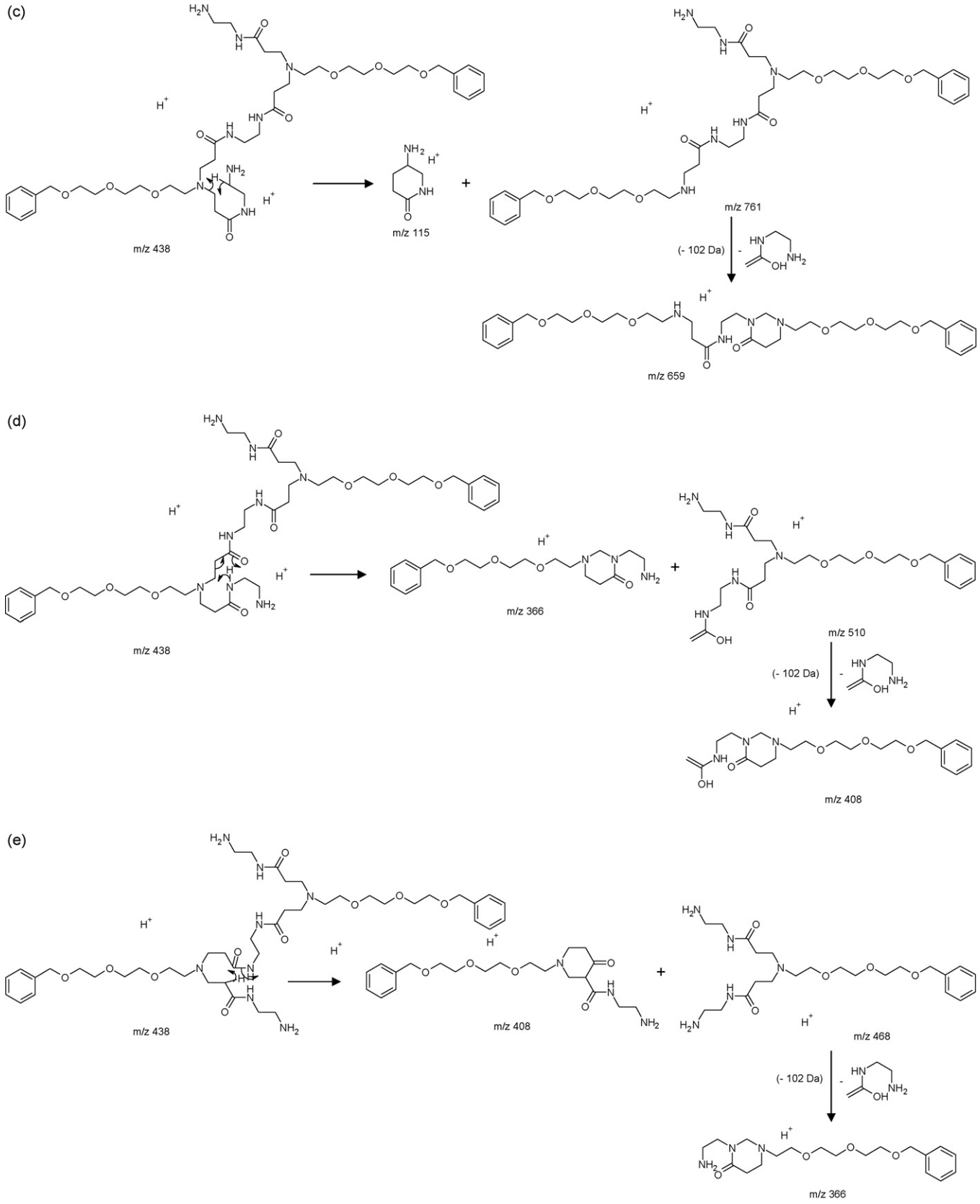

Scheme 5. (*Continued*).

from the structure of this daughter ion. Indeed, no peak was observed at *m/z* 264. Alternatively, *m/z* 366 would eliminate a 5-aminopiperidin-2-one molecule (114 Da) as described in Scheme 4b. As for the two previous cases, a benzylium ion was detected at *m/z* 91.

Collision-induced dissociation of the doubly protonated dimer was shown to produce a large number of daughter ions (Fig. 3). Two groups of primary reactions could be distinguished based on the charge state of the product ions. Mechanisms involved in the first group would produce two singly charged molecules and are described in Scheme 5. Amongst product ions shown in Scheme 5, those singly charged molecules which still possess an intact arm should be expected to consecutively eliminate the 102 Da enol, according to the mechanism described in Scheme 3a. Ions at *m/z* 683, *m/z* 671, *m/z* 659, *m/z* 408 and *m/z* 366 were thus considered to arise from such a dissociation of *m/z* 785, *m/z* 773, *m/z* 761, *m/z* 510 and *m/z* 468, respectively. The structure proposed for *m/z* 785 in Scheme 5a would allow this 102 Da neutral loss to proceed twice, as indicated by the peak observed at *m/z* 581. Amongst these ions, *m/z* 468 and *m/z* 683 were shown to eliminate a water molecule to yield low abundance peaks at *m/z* 450 and *m/z* 665, respectively. Although the structure proposed for these singly charged primary fragments would allow a consecutive elimination of the 114 Da neutral as depicted in Scheme 3b, data from the MS/MS spectrum in Fig. 3 indicate only *m/z* 785 might do so. Moreover, as mentioned before, elimination of 5-aminopiperidin-2-one was observed to proceed slower than the 102 Da enol loss. Therefore, the low abundance *m/z* 671 ion would mostly result from the consecutive dissociation of *m/z* 773 (Scheme 5b). The second group of dissociation reactions of the doubly protonated dimer would produce doubly charged fragments observed as the most intense peaks in the MS/MS spectrum. These reactions would mainly proceed through the loss of 1-(2-aminoethylamino)ethanol (102 Da) and water molecules. The ion at *m/z* 387 would be the doubly protonated homologue of *m/z* 773 shown in Scheme 5b and would further eliminate a second 102 Da neutral or a water molecule to yield *m/z* 378 or *m/z* 336 doubly charged molecules, respectively. Alternatively, a deshydratation of *m/z* 438 would lead to *m/z* 429, which will further eliminate the 102 Da molecule (yielding the doubly charged *m/z* 378) or water as a neutral to produce *m/z* 420.

3.2. PAMAM generation 1

Mass spectrometry of PAMAM generation 1 showed a major signal for ionized G_1NH_2 perfect dendrimer. In MALDI, the singly protonated molecule was detected at *m/z* 925, together with lower abundance sodium and potassium adducts at *m/z* 947 and *m/z* 963, respectively. Both singly and doubly charged G_1NH_2 were detected in ESI. Tandem mass spectrometry was performed on the protonated G_1NH_2. As shown in Fig. 4, each peak could be related to other ones by a 102 Da and/or a 114 Da mass difference. Since the precursor ion has two pairs of arms, mechanisms proposed in Scheme 3 would account for the four following loss series which ultimately lead to *m/z* 492:

- 102 Da followed by 114 Da (Scheme 3a) from the first pair, then the same neutral loss sequence from the second pair, i.e., an ion filiation such as *m/z* 924 → *m/z* 822 → *m/z* 708 → *m/z* 606 → *m/z* 492;
- 102 Da from both pairs, then 114 Da from both pairs, i.e., a fragmentation sequence such as *m/z* 924 → *m/z* 822 → *m/z* 720 → *m/z* 606 → *m/z* 492;
- 114 Da followed by 102 Da from the first pair (Scheme 3b), then the same neutral loss sequence from the second pair, i.e., an ion filiation such as *m/z* 924 → *m/z* 810 → *m/z* 708 → *m/z* 594 → *m/z* 492;
- 114 Da from both pairs, then 102 Da from both pairs, i.e., a fragmentation sequence such as *m/z* 924 → *m/z* 810 → *m/z* 696 → *m/z* 594 → *m/z* 492.

Although not observed in the MS/MS spectrum of protonated G_0NH_2, each arm should allow two *N*-(2-aminoethyl)acrylamide (114 Da) losses according to the first

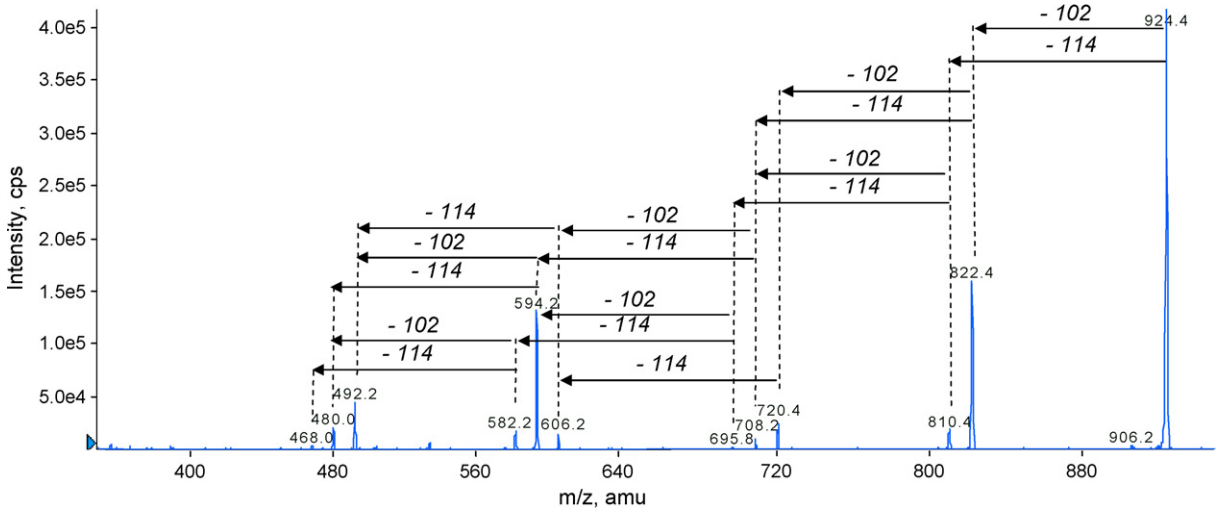

Fig. 4. ESI-MS/MS spectrum of the protonated G_1NH_2 (collision energy: 50 eV; laboratory frame).

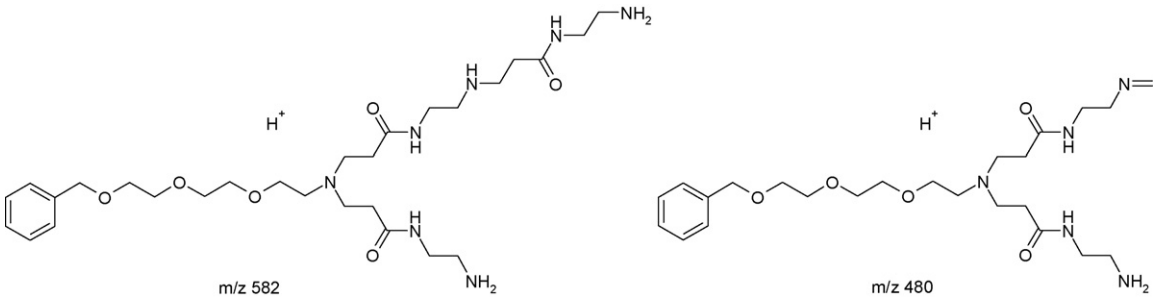

Scheme 6. Structure of daughter ions at *m/z* 480 and *m/z* 582 which would imply three 114 Da neutral losses in the dissociation sequence of *m/z* 924.

reaction step in Scheme 3b. Combination of up to four 114 Da neutral with 102 Da neutral losses would thus explain the presence of *m/z* 468 (i.e., protonated G_0NH_2) and *m/z* 480 and *m/z* 582 (see structures in Scheme 6) in the MS/MS spectrum of *m/z* 924.

Additional signals were observed in the mass spectra of PAMAM generation 1. Two series of adducts, observed from both ionization techniques, indicated the presence of two compounds with molecular weight of 809 Da and 863 Da, which were respectively identified as "missing arm" and "molecular loop" defects resulting from side reactions during the synthesis of G_1NH_2 from G_0NH_2. A dissociation sequence comprising one 102 Da loss followed by four 114 Da losses was observed from the protonated "missing arm" precursor at *m/z* 810 to ultimately lead a fragment ion at *m/z* 252 which structure was presented in Scheme 3. This MS/MS behaviour indicated the lack of an arm as compared to the perfect G_1NH_2 molecule. The expected dissociation sequence is stopped after two consecutive 102 Da neutral losses from the protonated "molecular loop" precursor at *m/z* 864, indicating only two arms were available for fragmentation. Moreover, an alternative dissociation pathway would consist of the elimination of the whole primary arm terminated by the loop. In contrast to the previous defects, the "dimer" was only detected in MALDI as sodium and potassium adducts. Other small peaks were observed in the mass spectra, indicating ionization of three compounds which molecular weight could be determined to be respectively 407, 581 and 695 Da based on multiple adducts detected for each molecule. The 407 Da compound could be the "molecular loop" defect already observed in generation 0 PAMAM sample. This defective molecule would have remained unreactive during the iterative step from generations 0 to 1. The presence of the two other compounds could be explained from two different reactions of the "missing arm" molecule present in generation 0 sample. This defective molecule would produce two different impurities in generation 1 depending on the ability of the amine group affected by the defect to react during the iterative synthesis. This hypothesis is illustrated in Fig. 5. The "missing arm" molecule could react (i) in a regular way (further called "normal growth") which would result in the branching of three new arms to yield a 695 Da compound and (ii) in an anomalous way (further called "blocked growth") in which no arm could be branched at the defect site, yielding a 581 Da molecule with only two new arms. It should also be noted from Fig. 5 that a "missing arm" defect which has occurred during the synthesis of the *n*th generation dendrimer and further undergone a "normal growth" will have, in the $(n+1)$th generation sample, a different structure, and thus a different mass, as compared to G_nNH_2 being affected by the "missing arm" defect during the synthesis of the $(n+1)$th generation. This statement can be applied to any of the considered side reactions. As long as molecules present in a dendrimer sample are able to react during the divergent synthesis, new impurities would be created in each dendrimer generation as the result of defect propagation in regular or defective ways. Since purification is usually not performed in such divergent dendrimer synthesis, mass spectral interpretation would rapidly become extremely tedious. A model was thus built to calculate molecular weight of expected structures which could be produced in each dendrimer generation for each side reaction.

3.3. Predictive models of structural deviations

To build these models, the following assumptions have been made from results obtained for the lowest generation dendrimer samples:

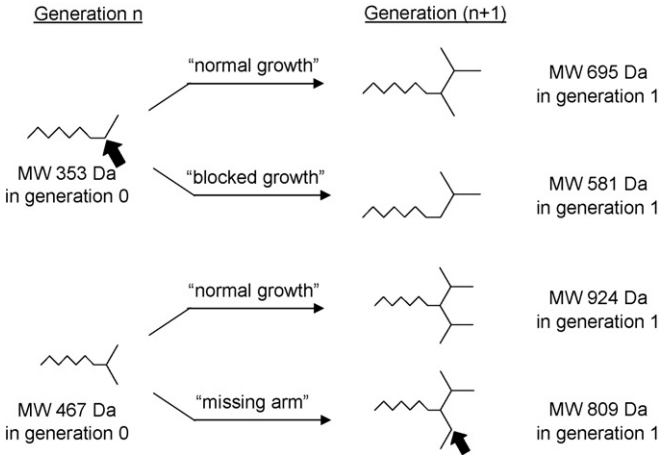

Fig. 5. Different evolutions of the "missing arm" molecule depending on the reactivity of the defected site (indicated by the black arrow). Note that, from generations *n* to $(n+1)$, the "normal growth" of the "missing arm" impurity would yield a different product as compared to the molecule obtained from the side reaction "missing arm" applied to the perfect molecule.

1. Once created, amine groups involved in a "molecular loop" would not further react during the iterative steps.
2. Once a molecule has suffered from a defect, it will not further be affected by any defect. This assumption seems to be reasonable with regard to the apparent low yield of side reactions: a recurrently defective molecule would be present at trace levels and might remain undetected.
3. The "dimer" defect does not further propagate.

The molecular weight, M_n, of a perfect molecule in the generation n dendrimer sample is given by the following equation:

$$M_n = 239.1521 + 114.0793 \left[\sum_{i=0}^{n} 2^{i+1} \right] \quad (1)$$

where 114.0793 is the accurate mass calculated for $C_5H_{10}N_2O$, the group of atoms in each new arms, and 239.1521 is the accurate mass of the dendrimer precursor.

From Eq. (1), the molecular weight, M_n, of any molecule in the nth generation dendrimer sample could be expressed as a function of j, the generation number at which this molecule has suffered from a defect as follows:

Table 1
Molecular weight, M_n, of expected molecules in generation n dendrimer sample (n from 0 to 3) calculated from Eqs. (1)–(4) where j is the generation number at which a given defect is produced

Defect	$j=0$	$j=1$	$j=2$	$j=3$
"No defect" (perfect molecule)				
M_0	467.3			
M_1		923.6		
M_2			1836.3	
M_3				3661.5
"Molecular loop"				
M_0	407.3			
M_1	407.3	863.6		
M_2	407.3	1319.9	1776.3	
M_3	407.3	2232.6	3145.2	3601.5
"Missing arm" + "normal growth"				
M_0	353.2			
M_1	695.5	809.5		
M_2	1379.9	1608.1	1722.2	
M_3	2748.9	3205.2	3433.4	3547.5
"Missing arm" + "blocked growth"				
M_0	353.2			
M_1	581.4	809.5		
M_2	1037.7	1494.0	1722.2	
M_3	1950.3	2863.0	3319.3	3547.5

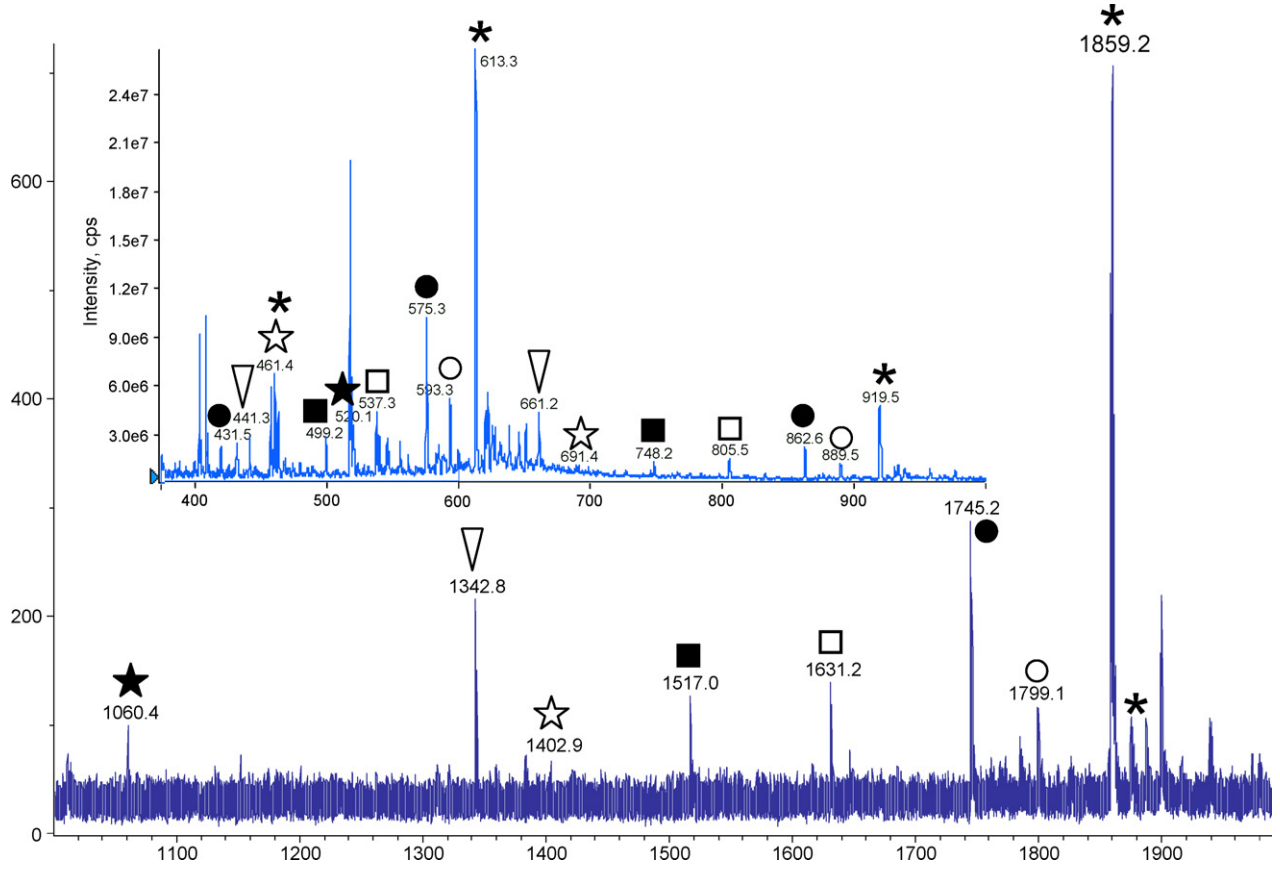

Fig. 6. MALDI and ESI (inset) mass spectra obtained for generation 2 dendrimer sample (laser fluence: 45%, number of shots: 100). Adduct of a same molecule are indicated by the same symbol in both spectra (asterisk: G_2NH_2; open circle: "molecular loop" defect created in generation 2; black circle: "missing arm" defect created in generation 2; open square: "normal growth" of the "missing arm" defect created in generation 1; black square: "blocked growth" of the "missing arm" defect created in generation 1; open star: "normal growth" of the "missing arm" defect created in generation 0; black star: "blocked growth" of the "missing arm" defect created in generation 0; open triangle: "molecular loop" defect created in generation 1).

- for the "molecular loop" defect:

$$M_n = 239.1521 + 114.0793 \times \left[\left(\sum_{i=0}^{j+1} 2^i\right) - 1 + (2^{j+2} - 4)\sum_{i=0}^{n-j-1} 2^i\right] - 60 \quad (2)$$

- for the "missing arm" defect followed by "normal growth":

$$M_n = 239.1521 + 114.0793 \times \left[\left(\sum_{i=0}^{j} 2^i\right) - 1 + (2^{j+1} - 1) + (2^{j+2} - 1)\sum_{i=0}^{n-j-1} 2^i\right] \quad (3)$$

- for the "missing arm" defect followed by "blocked growth":

$$M_n = 239.1521 + 114.0793 \times \left[\left(\sum_{i=0}^{j} 2^i\right) - 1 + (2^{j+1} - 1)\sum_{i=0}^{n-j-1} 2^i\right] \quad (4)$$

These four equations were then used to build a small database (Table 1) to be used as a guide for MS data interpretation up to generation 3 PAMAM dendrimer.

3.4. PAMAM generations 2 and 3

MALDI and ESI mass spectra of generation 2 PAMAM dendrimer are presented in Fig. 6. The perfect molecule G_2NH_2 yielded the most intense signal with both ionization techniques. It was detected as sodium (major peak) and potassium (minor peak) adducts in MALDI and as three different ions due to multiple protonation (from +2 to +4 charge state) in ESI. Apart from "dimer" formation, side reactions expected to affect G_1NH_2 were shown to occur. The "molecular loop" and the "missing arm" were detected as sodium adducts in MALDI at *m/z* 1799 and *m/z* 1745, respectively. ESI data also showed these defects to be present in the dendrimer sample: the "molecular loop" was observed as a doubly (*m/z* 889) and triply (*m/z* 593) protonated molecule while the "missing arm" was distributed in three charge states at *m/z* 863 (+2), *m/z* 575 (+3) and *m/z* 432 (+4). Additional peaks could be identified based on values from Table 1. The "missing arm" defect created in generation 1 would have propagated in generation 2 sample following either a "normal growth" or a "blocked growth", as respectively indicated by peaks at *m/z* 1631 and *m/z* 1517 in MALDI mass spectrum. These impurities were also observed after ESI as multi-protonated molecules (Fig. 6). Both ionization techniques also allowed the detection of signals which could be attributed to species resulting from either "normal growth" or "blocked growth" propagation of the "missing arm" defect created in generation 0. Finally, peaks at *m/z* 1343 in MALDI and at *m/z* 661 and *m/z* 441 in ESI would indicate the presence

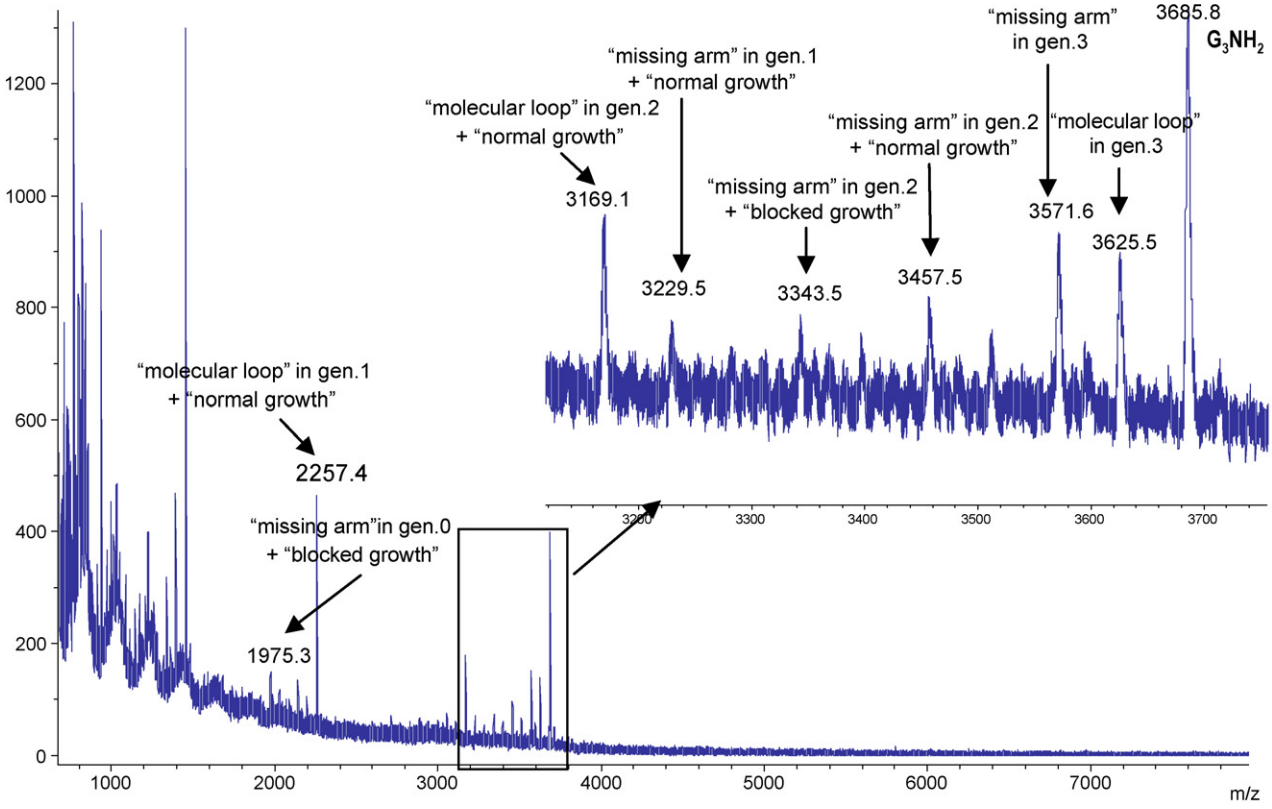

Fig. 7. MALDI mass spectrum obtained for generation 3 dendrimer sample (laser fluence: 46%; number of shots: 400). Inset: expanded view of the mass spectrum in the range *m/z* 3000–3800.

of the intact "molecular loop" created in generation 1. Numerous other peaks, amongst which some intense ones, could not be accounted for in the ESI mass spectrum. This would indicate additional unknown side reactions would occur. However, MALDI homologues of these ESI ions were not observed. Structure of these ions will be explored in a forthcoming MS/MS study.

Generation 3 PAMAM sample was mass analyzed using both ionization techniques and MALDI data are presented in Fig. 7. ESI mass spectrum (data not shown) is very complicated due to multiple charging of the molecules (from +4 to +6 charge states) and low-resolution mass analysis. During the iterative dendrimer synthesis sequence, the growth of G_2NH_2 yielded the expected G_3NH_2 (observed as a sodium adduct at *m/z* 3686) but was also affected by side reactions, resulting in the formation of the "missing arm" and "molecular loop" defects, respectively detected as sodium adducts at *m/z* 3572 and *m/z* 3626. Additional impurities present in generation 3 dendrimer sample could be classified according to the generation number at which the defect they arise from was created. The "molecular loop" and "missing arm" produced during generation 2 synthesis, would have further propagated to yield new impurities: "normal growth" of these defects was indicated by peaks at *m/z* 3169 and *m/z* 3458, respectively, while the *m/z* 3344 ion would result from the "blocked growth" of the "missing arm". Based on data from Table 1, peaks observed at *m/z* 2257 and *m/z* 3230 could, respectively be attributed to impurities (ionized as sodium adducts) resulting from a "normal growth", up to generation 3, of "molecular loop" and "missing arm" produced during generation 1 synthesis. Finally, the "missing arm" defect created in generation 0 would have propagated in a "blocked growth" way up to the third generation, as indicated by the sodium adduct detected at *m/z* 1975 in Fig. 7.

4. Conclusion

MS analysis of fan-shape PAMAM dendrimer samples was performed in both MALDI and ESI. Although most molecules could be detected in both ionization techniques, MALDI and ESI did not allow the same conclusions to be reached regarding sample composition. Tandem mass spectrometry of protonated perfect structures showed favoured dissociations almost exclusively proceeded via combined losses of 5-aminopiperidin-2-one (114 Da) and 1-(2-aminoethylamino)ethanol (102 Da) neutrals, formed from free arms of the dendrimers. Any deviations from these specific fragmentation pathways allowed structural defects to be characterized. In addition to the commonly reported "missing arm" and "molecular loop", new impurities were detected from generation 1 dendrimer sample. They would arise from propagation, in a given generation *n* sample, of defects created during the synthesis of lower generation dendrimers. Based on the different ways defects were shown to propagate, predictive models were built to guide peak assignment in MALDI and ESI mass spectra and allowed the most intense ions to be identified in high generation samples. Some signals still remained unknown. Further MS/MS study will be performed on these ions to characterize their structure and possibly determine their origin.

Acknowledgment

We wish to express our acknowledgments to Spectropole, the Analytical Facility of Aix-Marseille Universities, for technical support to this study by allowing special access to the instruments.

References

[1] D.A. Tomalia, A.M. Naylor, W.A. Goddard, Angew. Chem. Int. Ed. 29 (1990) 138.
[2] A.W. Bosman, H.M. Janssen, E.W. Meijer, Chem. Rev. 99 (1999) 1665.
[3] J.M.J. Frechet, J. Polym. Sci., Part A: Polym. Chem. 41 (2003) 3713.
[4] D.A. Tomalia, B. Huang, D.R. Swanson, H.M. Brothers, J.W. Klimash, Tetrahedron 59 (2003) 3799.
[5] D.A. Tomalia, Prog. Polym. Sci. 30 (2005) 294.
[6] C.J. Hawker, J.M.J. Frechet, J. Am. Chem. Soc. 112 (1990) 7638.
[7] J.W. Weener, J.L.J. van Dongen, E.W. Meijer, J. Am. Chem. Soc. 121 (1999) 10346.
[8] S. Svenson, D.A. Tomalia, Adv. Drug Delivery Rev. 57 (2005) 2106.
[9] D.A. Tomalia, Macromol. Symp. 101 (1996) 243.
[10] G.J. Kallos, D.A. Tomalia, D.M. Hedstrand, S. Lewis, J. Zhou, Rapid Commun. Mass Spectrom. 5 (1991) 383.
[11] A. Ebber, M. Vaher, J. Peterson, M. Lopp, J. Chromatogr. A 949 (2002) 351.
[12] X.Y. Shi, I. Banyai, M.T. Islam, W. Lesniak, D.Z. Davis, J.R. Baker, L.P. Balogh, Polymer 46 (2005) 3022.
[13] L.P. Tolic, G.A. Anderson, R.D. Smith, H.M. Brothers, R. Spindler, D.A. Tomalia, Int. J. Mass Spectrom. 165 (1997) 405.
[14] L. Zhou, D.H. Russell, M.Q. Zhao, R.M. Crooks, Macromolecules 34 (2001) 3567.
[15] J. Peterson, V. Allikmaa, J. Subbi, T. Pehk, M. Lopp, Eur. Polym. J. 39 (2003) 33.
[16] A.M. Caminade, R. Laurent, J.P. Majoral, Adv. Drug Deliver. Rev. 57 (2005) 2130.
[17] L.J. Hobson, W.J. Feast, Polymer 40 (1999) 1729.
[18] R. Muller, G. Allmaier, Rapid Commun. Mass Spectrom. 20 (2006) 3803.
[19] J.H. Zhou, J.Y. Wu, X.X. Liu, F.Q. Qu, M. Xiao, Y. Zhang, L. Charles, C.C. Zhang, L. Peng, Org. Biomol. Chem. 4 (2006) 581.
[20] J.C. Hummelen, J.L.J. vanDongen, E.W. Meijer, Chem. Eur. J. 3 (1997) 1489.
[21] S. van der Wal, Y. Mengerink, J.C. Brackman, E.M.M. de Brabander, C.M. Jeronimus-Stratingh, A.P. Bruins, J. Chromatogr. A 825 (1998) 135.
[22] J. de Maaijer-Gielbert, C.G. Gu, A. Somogyi, V.H. Wysocki, P.G. Kistemaker, T.L. Weeding, J. Am. Soc. Mass Spectrom. 10 (1999) 414.
[23] B.B. Baytekin, N. Werner, F. Luppertz, M. Engeser, J. Bruggemann, S. Bitter, R. Henkel, T. Felder, C.A. Schalley, Int. J. Mass Spectrom. 249 (2006) 138.
[24] I.A. Mowat, R.J. Donovan, M. Bruce, W.J. Feast, N.M. Stainton, Eur. Mass Spectrom. 4 (1998) 451.
[25] A.J. Clark, A.A. Coleshill, D.M. Haddleton, S.J. Isles, H.S. Sahota, P.C. Taylor, S.G. Yeates, Eur. Mass Spectrom. 5 (1999) 273.
[26] C. Kim, H. Kim, C.R. Chim. 7 (2004) 503.
[27] Z.C. Wu, K. Biemann, Int. J. Mass Spectrom. 165 (1997) 349.
[28] C. Kim, K.I. Lim, C.G. Song, J. Organomet. Chem. 690 (2005) 3278.
[29] A. Krupkova, J. Cermak, Z. Walterova, J. Horsky, Anal. Chem. 79 (2007) 1639.
[30] F.R.F. Fan, C.L. Mazzitelli, J.S. Brodbelt, A.J. Bard, Anal. Chem. 77 (2005) 4413.
[31] A. Mazzaglia, L.M. Scolaro, D. Garozzo, P. Malvagna, R. Romeo, J. Organomet. Chem. 690 (2005) 1978.
[32] B.L. Schwartz, A.L. Rockwood, R.D. Smith, D.A. Tomalia, R. Spindler, Rapid Commun. Mass Spectrom. 9 (1995) 1552.

[33] S.A. McLuckey, K.G. Asano, T.G. Schaaff, J.L. Stephenson, Int. J. Mass Spectrom. 196 (2000) 419.
[34] C.L. Mazzitelli, J.S. Brodbelt, J. Am. Soc. Mass Spectrom. 17 (2006) 676.
[35] A. Adhiya, C. Wesdemiotis, Int. J. Mass Spectrom. 214 (2002) 75.
[36] M. He, S.A. McLuckey, Rapid Commun. Mass Spectrom. 18 (2004) 960.
[37] J. Subbi, R. Aguraiuja, R. Tanner, V. Allikmaa, M. Lopp, Eur. Polym. J. 41 (2005) 2552.
[38] J.C. Blais, C.O. Turrin, A.M. Caminade, J.P. Majoral, Anal. Chem. 72 (2000) 5097.